environments

MDPI

Article

Pulse of the Storm: 2024 Hurricane Helene's Impact on Riverine Nutrient Fluxes Across the Oconee River Watershed in Georgia

Arka Bhattacharjee [1,†,‡], Grace Stamm [2,3,†], Blaire Myrick [4], Gayatri Basapuram [2], Avishek Dutta [2,5,*] and Srimanti Duttagupta [2,*]

1 School of Computing, University of Georgia, Athens, GA 30602, USA; arkabofficial@gmail.com
2 Department of Geology, University of Georgia, Athens, GA 30602, USA; grace.stamm@uga.edu (G.S.); gayatri.basapuram@uga.edu (G.B.)
3 Department of Physics and Astronomy, University of Georgia, Athens, GA 30602, USA
4 Department of Anthropology, University of Georgia, Athens, GA 30602, USA; blaire.myrick@uga.edu
5 Savannah River Ecology Laboratory, University of Georgia, Aiken, SC 29802, USA
* Correspondence: avishek.dutta@uga.edu (A.D.); sduttagupta@uga.edu (S.D.)
† These authors contributed equally to this work.
‡ Current address: H. Milton Stewart School of Industrial and Systems Engineering, Georgia Institute of Technology, Atlanta, GA 30332, USA.

Abstract

Tropical cyclones can rapidly alter watershed chemistry by shifting hydrologic pathways and mobilizing stored nutrients, yet these disturbances often remain undetected when storms cause little visible flooding or geomorphic damage. During Hurricane Helene 2024, intense rainfall across the Oconee River watershed in Georgia generated sharp increases in discharge that triggered substantial nutrient export despite minimal physical alteration to the landscape. High-frequency measurements of nitrate, phosphate, and sulfate in urban, forested, and recreational settings revealed pronounced and synchronous post-storm increases in all three solutes. Nitrate showed the strongest and most persistent response, with mean concentrations increasing from approximately 1–3 mg/L during pre-storm conditions to 6–14 mg/L post-storm across sites, and remaining elevated for several months after hydrologic conditions returned to baseline. Phosphate concentrations increased sharply during the post-storm period, rising from pre-storm means of $\leq$0.3 mg/L to a post-storm average of 1.5 mg/L, but declined more rapidly during recovery, consistent with sediment-associated mobilization and subsequent attenuation. Sulfate concentrations also increased substantially across the watershed, with post-storm mean values commonly exceeding 20 mg/L and maximum concentrations reaching 41 mg/L, indicating sustained dissolved-phase release and enhanced temporal variability. Recovery trajectories differed by solute: phosphate returned to baseline within weeks, nitrate declined gradually, and sulfate remained elevated throughout the winter. These findings demonstrate that substantial chemical perturbations can occur even in the absence of visible storm impacts, underscoring the importance of event-based, high-resolution monitoring to detect transient but consequential shifts in watershed biogeochemistry. They also highlight the need to better resolve solute-specific pathways that govern nutrient mobilization during extreme rainfall in mixed-use watersheds with legacy nutrient stores and engineered drainage networks.

Keywords: hurricane; storm-driven nutrient transport; event-based monitoring; nutrient release; runoff; mobilization

Check for updates

Academic Editor: Chihhao Fan

Received: 8 December 2025
Revised: 24 January 2026
Accepted: 27 January 2026
Published: 1 February 2026

Copyright: © 2026 by the authors. Licensee MDPI, Basel, Switzerland. This article is an open access article distributed under the terms and conditions of the Creative Commons Attribution (CC BY) license.

1. Introduction

Tropical cyclones are increasingly recognized not only for their destructive potential to infrastructure and communities, but also for their capacity to induce rapid and significant alterations in watershed-scale hydrology and biogeochemistry [1,2]. High-intensity, short-duration rainfall associated with these events can rapidly expand hydrologic connectivity, mobilize stored solute pools, and alter surface–subsurface exchange [3,4]. As a result, large pulses of water, sediment, and dissolved constituents are often transmitted through river networks in timeframes spanning hours to days [5]. These hydrologic perturbations can disrupt established nutrient transport pathways, shift dominant biogeochemical processes, and restructure aquatic chemistry at spatial scales that extend far beyond the storm footprint [6]. While the physical consequences of hurricanes, such as coastal flooding, channel erosion, and wind damage, are well documented, chemical responses in inland freshwater systems are less visible and therefore less frequently measured, where storms do not produce dramatic geomorphic change [7,8]. The influence of tropical cyclones on nutrient mobilization, transformation, and export in riverine systems remains incompletely characterized [9,10].

Extreme precipitation and tropical cyclones can propagate hydrologic and sedimentary impacts well beyond inland watersheds, influencing estuarine and coastal systems through enhanced sediment, nutrient, and freshwater delivery. Previous studies have documented storm-driven coastal flooding, and barrier breaching processes, as well as sediment transport and channel erosion associated with storm surge and wave–current interactions in nearshore environments [11–13]. Compound flooding driven by the interaction of storm surge, river discharge, and precipitation further amplifies downstream impacts during tropical cyclones [14]. Previous studies highlight the importance of viewing storm impacts as part of a coupled inland–coastal continuum, in which watershed-scale hydrologic and biogeochemical responses influence downstream estuarine and coastal dynamics (Table 1). Within this broader framework, the present study focuses on resolving storm-driven nutrient responses within an inland mixed-use watershed, providing upstream context for downstream coastal and estuarine impacts during extreme events.

Table 1. Prior studies documenting storm-driven hydrologic and biogeochemical export across diverse aquatic systems.

Study	Storm/Event	Location	System Type	Solutes Assessed	Sampling Design	Key Findings Relevant to Storm-Driven Export
Paerl et al., 2018 [9]	Hurricane Florence	North Carolina, USA	River–estuary continuum	N, P, C	High frequency + discrete	Extreme nutrient and carbon loading driven by compound flooding; delayed estuarine recovery lasting months
Vidon et al., 2018 [1]	Hurricane Irene	Northeastern USA	Forested watershed	DOC, nutrients	Event-based sampling	Single storm exported a disproportionate fraction of annual dissolved organic matter and nutrients
Cai et al., 2013 [10]	Hurricanes Gustav (2008) and Ike (2008)	Lower Pearl River Estuary, China	Large tropical river–estuary system	Major ions, nutrients (NO_3^-, NH_4^+, PO_4^{3-}), dissolved organic carbon (DOC), particulate matter	High-frequency river and estuarine sampling before, during, and after hurricane passage	Tropical cyclones caused sharp increases in river discharge, leading to enhanced export of nutrients, DOC, and particulates to the estuary; storm pulses altered solute concentrations and fluxes more strongly than seasonal variability, demonstrating that extreme events dominate short-term material export from large river systems

Table 1. *Cont.*

Study	Storm/Event	Location	System Type	Solutes Assessed	Sampling Design	Key Findings Relevant to Storm-Driven Export
Gori et al., 2020 [14]	Tropical cyclones	Coastal USA	Coupled river–coastal system	Water levels, nutrients	Observations + modeling	Compound flooding from rainfall, surge, and discharge amplified downstream impacts
Plomaritis et al., 2018 [11]	Extreme storms	Portugal	Coastal barrier systems	Sediment-associated nutrients	Event-scale analysis	Storm overwash and breaching redistributed sediment and nutrients
Nienhuis et al., 2021 [13]	Extreme storms	Global	Coastal barriers	Sediment, phosphorus	Numerical modeling	Storms controlled barrier breaching and overwash, altering coastal sediment–nutrient pathways
Ma et al., 2024 [15]	Storm surge	China coast	Estuarine–nearshore	Sediment, nutrients	Coupled hydro-morphodynamic model	Storm surge enhanced bed erosion and nutrient release under wave–current interaction

Hurricane Helene made landfall in Florida's Big Bend region as a Category 4 storm in September 2024 and tracked inland across the Southeastern United States [16,17]. The Oconee River watershed in Georgia, USA, received intense rainfall during the storm's passage, resulting in rapid increases in discharge and gage height throughout the basin [18]. Despite these hydrologic responses, Athens-Clarke County, a population and infrastructure center within the watershed, reported minimal disruption to power, transportation, or public health systems. From a public and municipal standpoint, the region was viewed as having experienced limited storm impact. However, outward stability of infrastructure does not directly translate to biogeochemical stability. Storm-driven hydrologic connectivity can mobilize terrestrial nutrient pools, trigger redox transitions in soils and sediments, and shift the relative contributions of groundwater, shallow subsurface flow, and surface runoff to stream chemistry [19]. Such chemical reorganization can proceed even when channels do not overtop their banks and when floodplain inundation is absent [20]. The apparent absence of disturbance therefore obscures subtler hydrologic and geochemical perturbations operating within the watershed.

Storm-induced changes in flow regime exert substantial control over nutrient mobilization processes, specifically for solutes that exhibit strong coupling to hydrologic pathways [21]. Nitrate (NO_3^-), phosphate (PO_4^{3-}), and sulfate (SO_4^{2-}) are responsive to short-term increases in runoff, soil leaching, sediment resuspension, and erosion of particulate-bound material [4,22]. For nitrate, elevated discharge can flush mineralized soil nitrogen, shallow groundwater stores, and urban stormwater infrastructure, increasing delivery to streams on rapid timescales [23]. Phosphate can be mobilized through multiple storm-activated pathways, including desorption from mineral surfaces under transient redox conditions, scouring of phosphorus-rich sediments, and transport of particulate organic matter [24]. Sulfate may respond through oxidation of reduced sulfur species, leaching of soil sulfate pools, and transport through engineered urban drainage networks [25]. Pulse-like increases in these ions can alter aquatic productivity, shift redox conditions in the water column and sediments, and modify downstream nutrient loading to reservoirs, wetlands, and estuarine systems [26]. These consequences are relevant in watersheds that contain heterogeneous land cover, legacy nutrient storage, and engineered hydrologic infrastructure [27,28].

The Oconee River watershed integrates urban development, agricultural land, and forested areas, producing spatially variable source pools of dissolved and particulate nutrients [29,30]. The co-occurrence of land use increases the sensitivity of the watershed

to hydrologic forcing and makes it an informative case study for storm-driven chemical perturbation. Prior to Hurricane Helene, riverine chemistry in the watershed was stable and reflected typical seasonal variability in discharge, temperature, and biogeochemical cycling [31–33]. The storm presented a natural experiment in which a significant hydrologic disturbance occurred without visible flood damage or infrastructure failure, allowing direct assessment of chemical change independent of geomorphic disruption.

This study assessed the hydrological and biogeochemical responses of the Oconee River watershed to Hurricane Helene (2024) using event-focused, high-temporal-resolution discrete sampling of surface waters across spatially distributed monitoring sites, integrated with discharge, precipitation, temperature, and gage-height data. Temporal changes in nitrate, phosphate, and sulfate concentrations before, during, and after the storm were assessed, with specific focus on (1) the magnitude of nutrient pulses associated with peak discharge; (2) spatial heterogeneity among urban, forested, and semi-lentic sub-watersheds; and (3) the duration and trajectory of recovery during the post-storm recession period. The present study interprets these chemical changes in the context of watershed land use, hydrologic routing, and sediment–water interactions to identify dominant nutrient mobilization pathways. The results demonstrate that substantial shifts in nutrient export can occur in inland river systems during high-intensity precipitation events, even when geomorphic change is minimal and societal disruption is limited. This work highlights the importance of integrated, event-responsive monitoring frameworks for detecting non-visible freshwater impacts of extreme weather events.

The study was conducted within the Oconee River watershed in north-central Georgia, a mixed-use basin consisting of urban, agricultural, and forested landscapes [34]. Sampling locations were selected to capture the range of land-use and hydrological conditions influencing nutrient transport across the watershed (Figure 1). Three of the sites, Firefly Trail (FT), River Mill (RM), and the Water Treatment Plant intake (WTP), are located along the North Oconee River. Lake Chapman in Sandy Creek recreational park (SC), by contrast, represents a recreational and lentic system within a park landscape, where slower water turnover and enhanced sediment interaction influence nutrient dynamics [29] (Table 2). These sites were chosen to capture both spatial heterogeneity and differing levels of anthropogenic influence. FT and RM are strongly urbanized reaches draining residential and commercial zones (Table 2). Oconee River near Oconee National Forest (OR) reflects a forested upstream setting with limited direct urban inputs and greater interaction with riparian vegetation and soil organic matter [29] (Table 2). OR integrates cumulative watershed inputs, and WTP lies immediately upstream of the municipal intake infrastructure. Hurricane Helene brought intense rainfall to the region in late September 2024, resulting in elevated flows but limited visible infrastructure damage. Despite the absence of flooding or community disruption, hydrological connectivity increased sharply, presenting an ideal natural experiment to evaluate storm-driven nutrient mobilization.

Table 2. Summary of monthly physicochemical parameters and hydrological metrics across the Oconee River watershed between January 2024 and March 2025.

		Jan 2024	Feb 2024	Mar 2024	Apr 2024	May 2024	Aug 2024	Sep 2024	Oct 2024	Nov 2024	Dec 2024	Jan 2025	Feb 2025	Mar 2025
pH	FT	6.4	7.1	8.3	8.4	8.1	7.9	7	7.7	7.9	7.5	7.5	7.3	7.4
	RM		7.1	7.9	7.9	8.2	8	7	7.8	8	7.6	7.6	7.20	7.3
	SC	7.9	7.9	8.1	8.4	8.1	8.9	8.4	8	8.5	8.5	8.1	8.00	7.9
	OR	6.6	7.3	8.4	8.8	9.7	9.5	8.6	9.3	5.5	7.1	7.1	7.20	7.5
	WTP	7	7.9	8.3	8.4	8	7.8	6.9	7.6	7.9	7.8	7.4	7.3	7.3

Table 2. *Cont.*

		Jan 2024	Feb 2024	Mar 2024	Apr 2024	May 2024	Aug 2024	Sep 2024	Oct 2024	Nov 2024	Dec 2024	Jan 2025	Feb 2025	Mar 2025
Temperature (°C)	FT	7.3	10.2	20	20	23.5	22.4	21.6	11.8	10.2	8.3	7.5	10.10	15.00
	RM		14.3	19.4	20	24	22.9	22.1	12.3	10.7	8.8	8	9.70	10.00
	SC	9.6	7.2	19.8	22	21.5	22.9	19.2	8.9	10.8	9.7	9.60	10.10	19.20
	OR	8.4	8.5	18.2	19	25.5	24.4	23.6	13.8	8.2	8.3	7.5	11.00	18.00
	WTP	7.9	8.4	18.7	21.2	23.4	22.3	21.5	11.7	10.1	8.2	7.4	9.40	13.00
DO (mg/L)	FT	6.1	5.9	3.6	3.3	3.1	3.4	6.8	5.1	5.3	5.5	5.8	5.50	5.4
	RM		3.9	4.2	3.6	3.9	7.3	6.3	5.8	6	6.3	6	5.40	5.5
	SC	6.7	6.8	6.4	6.9	6.8	6.8	6.2	5.9	5.5	5.7	5.6	5.80	5.4
	OR	7	6.2	4.5	3.2	5.1	5.4	7.8	7.1	5.9	5.5	5.8	6.10	6
	WTP	5.9	6.2	6.9	6.1	6.4	6.4	7.1	6.4	6.4	6.5	6.5	6.20	6.5
ORP (mV)	FT	214.6	159.9	148	218.9	207.8	152.7	161.5	188.5	159.7	152.8	199	201.90	213.1
	RM		147.2	183	194.4	219.4	208.3	153.2	175.1	189	160.2	153.3	148.5	145.0
	SC	160	162.5	164.9	163.7	162.9	159.7	121.1	169.5	150.7	149.7		152.6	159.2
	OR	267	145.2	186.1	192.5	220.9	209.8	154.7	176.6	186.5	159.7	152.8	154.6	146.6
	WTP	193	195	204	203	218.8	207.7	164.9	199.8	213.7	184.9	178	186.9	186.1
Turbidity (NTU)	FT	29.0	36.0	39.6	27.0	21.8	20.1	51.3	22.4	12.6	10.0	9.5	14.6	12.7
	RM		24.9	29.2	23.5	22.3	20.6	51.8	23.3	13.1	10.5	10.0	19.0	17.6
	SC	31.0	25.0	27.0	24.3	23.6	22.5	21.4	19.1	18.0	16.8	16.2	28.5	24.8
	OR	15.0	30.2	29.5	31.6	23.8	22.1	57.3	21.8	17.6	15.0	14.5	25.5	25.0
	WTP	24.9	20.8	29.4	23.6	21.7	20.0	38.2	9.3	9.8	9.9	9.4	11.8	10.3
Gage Height (ft)		8.01	6.14	6.12	4.78	4.71	3.40	8.12	4.11	4.37	4.99	4.78	5.04	5.23
Discharge (ft^3/s)		1125.0	586.0	579.0	202.0	189.0	45.9	1230.0	84.0	111.0	204.0	168.0	234.0	264.0
Precipitation (mm/day)		12.7	0	2.54	0	0.762	0	124.97	0	48.01	64.01	71.12	17.78	12.7

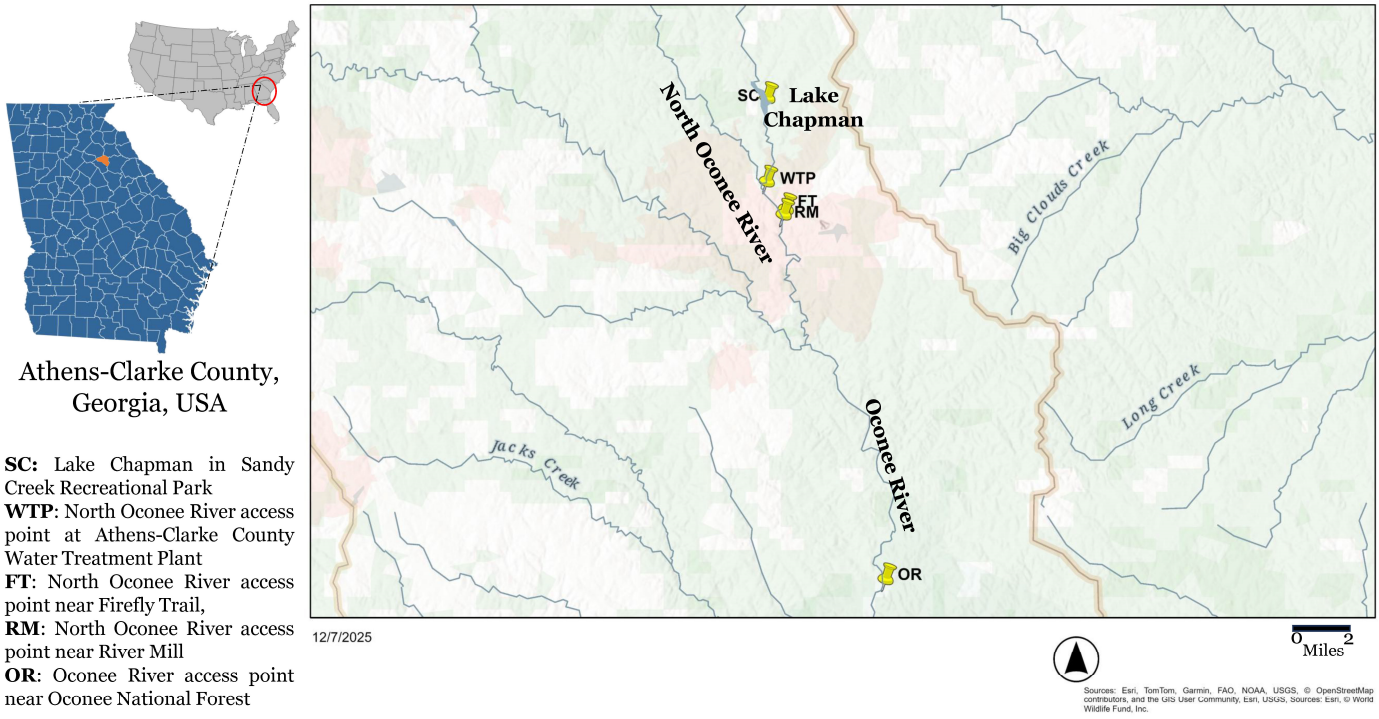


Figure 1. Map showing the study area in Georgia, USA, and sampling locations details across the Oconee River watershed. The pink shading represents developed/urban land cover, while white and pale green areas correspond to forested and low-intensity land cover, based on NLCD land-use classifications.

2. Methods

2.1. Sampling Design and Water Collection

Surface water samples were collected monthly from January 2024 through March 2025, spanning both pre-hurricane and post-hurricane hydrological regimes. Following Hurricane Helene (27 September 2024), the sampling frequency was increased to capture

rapid biogeochemical responses. The first post-storm sampling was conducted on 29 September 2024, approximately 48 h after the storm, followed by a second sampling event three weeks later in October 2024. After October 2024, samplings resumed on a monthly basis through March 2025. At each site, surface water was collected at the nearest accessible point, avoiding bank-inflow zones to minimize bank-edge dilution, using a telescopic sampler. Samples were collected in pre-baked and clean 1 L wide-mouth amber bottles and transported to the laboratory for immediate analysis [34]. Physicochemical parameters, including pH, dissolved oxygen (DO), oxidation-reduction potential (ORP), conductivity, and turbidity, were measured using a HANNA HI9829 multiparameter water quality probe (Hanna Instruments, Smithfield, Rhode Island, USA) (Table 2). The instrument was calibrated according to the manufacturer's instructions before each field sampling event to ensure accurate and reliable measurements.

2.2. Nutrient Analysis in River Water Samples

Concentrations of nitrate (NO_3^-), phosphate (PO_4^{3-}), and sulfate (SO_4^{2-}) were quantified using a Hanna Iris Visible Spectrophotometer (Hanna Instruments, Smithfield, RI, USA) with dedicated reagents for each analyte (HI93728-01 for nitrate, HI93713-01 for phosphate, and HI93751-01 for sulfate) [30]. All reagents were prepared according to the manufacturer's instructions, and separate calibration curves were generated for each ion before sample analysis to ensure accuracy across the concentration range encountered within the watershed. Calibration curves were verified at the beginning of each analytical session, and instrument performance was validated using nitrate, phosphate, and sulfate solutions. Each water sample was analyzed in triplicate to minimize analytical error, and any replicate with variability > 5% was rerun. Blanks and laboratory controls accompanied each run to detect contamination or drift. Final concentrations were computed as the average of replicate readings and reported in mg/L.

2.3. Hydrological and Meteorological Data Acquisition

Daily precipitation, discharge, gage height, and water temperature data were obtained from National Oceanic and Atmospheric Administration (NOAA) and United States Geological Survey (USGS) monitoring stations associated with the Oconee basin [35,36]. These hydrological datasets were used to contextualize short-term nutrient variability, particularly during the high-flow period immediately after the Hurricane. Increased discharge was used as a proxy for enhanced runoff and watershed connectivity.

2.4. Land Use and Watershed Characterization

Land-use classifications for each sampling site's drainage area were derived using Georgia Department of Natural Resources GIS layers and U.S. National Land Cover Database (NLCD) land cover datasets [37]. Sites were categorized by dominant land cover: urban, agricultural, forested, mixed, and interpreted in connection with nutrient responses [29]. Impervious cover and stormwater infrastructure data were also evaluated to understand hotspot nitrate and phosphate delivery during peak flows.

2.5. Data Analysis and Statistical Methods

Data visualization and statistical analysis were performed in R Studio (R v4.4.2). The "tidyverse" and "Hmisc" libraries were used to generate correlation matrices among nutrients, hydrology, and physicochemical properties, including dissolved oxygen, pH, ORP, turbidity, discharge, and gage height [38,39]. The "corrplot" package was used to visualize correlation structures and nutrient interaction networks. Descriptive statistics have been provided for nitrate, phosphate, and sulfate concentrations in the Supplementary Information (Supplementary Information-S1, Table S1).

3. Results

3.1. Hydrologic Context of the Post-Hurricane Period

Prior to Hurricane Helene, the Oconee watershed exhibited stable baseflow and low-to-moderate nutrient concentrations across all sampling locations, with minor seasonal fluctuations driven by temperature and normal rainfall patterns. Following the storm's landfall and passage over the region, daily discharge increased sharply, particularly along the North Oconee River, reflecting rapid catchment-to-stream connectivity. Although Athens-Clarke County did not experience visible flooding or infrastructure disruption, the hydrochemical signature of the watershed shifted immediately. Elevated flows persisted for several weeks and corresponded closely with dramatic changes in anion concentrations.

Across all five sites, nitrate, phosphate, and sulfate increased markedly after the Hurricane. Pre-storm variability was relatively low and largely aligned with land-use gradients. Urban reaches consistently exhibited higher nutrient concentrations than forested or semi-lentic locations. However, post-storm conditions no longer followed these predictable patterns. Concentrations surged simultaneously across urban, recreational, and forested settings, indicating a watershed-wide disturbance rather than isolated, site-specific anomalies. The results showed not only higher mean concentrations but also markedly greater variability in nutrient distributions during the post-storm period, as reflected by the increased interquartile ranges and expanded data spread in Figure 2, indicating enhanced temporal instability and episodic nutrient delivery (Table S1). The spatial and temporal variability of nitrate (NO_3^-), phosphate (PO_4^{3-}), and sulfate (SO_4^{2-}) across the Oconee River watershed was strongly modulated by site-specific land use, hydrological regimes, and the aftermath of Hurricane Helene (Figure 2, Table 3).

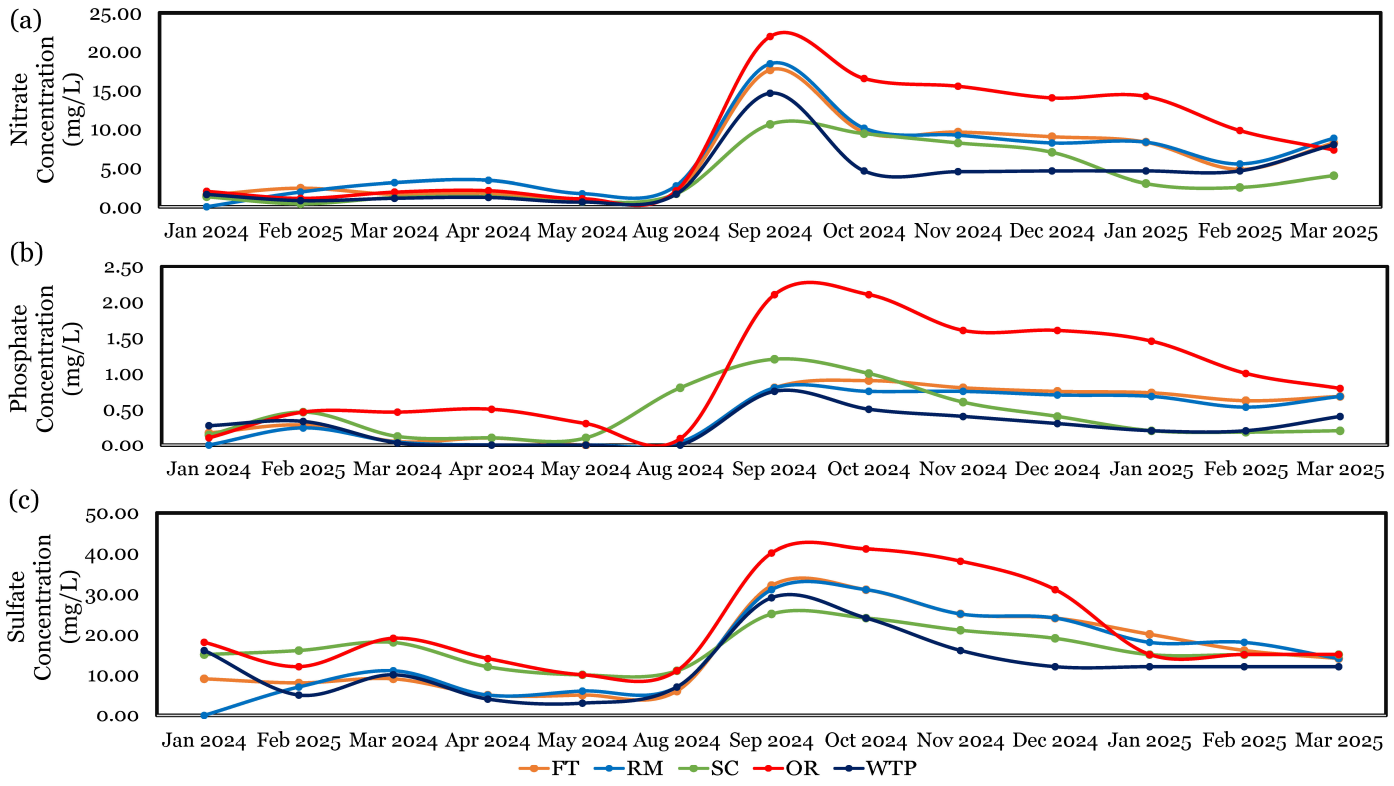


Figure 2. Temporal variation in (**a**) nitrate, (**b**) phosphate, and (**c**) sulfate concentrations (mg/L) measured across all sampling sites from January 2024 to March 2025. Each panel illustrates seasonal patterns and site-specific differences observed throughout the sampling period.

Table 3. Spatiotemporal distribution of nitrate, phosphate, and sulfate concentrations (mg/L) across the Oconee River watershed between Jan 2024 and Mar 2025.

Sampling Site	FT			RM			SC			OR			WTP		
	Nitrate	**Phosphate**	**Sulfate**	**Nitrate**	**Phosphate**	**Sulfate**	**Nitrate**	**Phosphate**	**Sulfate**	**Nitrate**	**Phosphate**	**Sulfate**	**Nitrate**	**Phosphate**	**Sulfate**
Jan 2024	1.50	0.17	9.00				1.30	0.14	15.00	2.00	0.10	18.00	1.60	0.27	16.00
Feb 2025	2.40	0.28	8.00	1.90	0.24	7.00	0.40	0.46	16.00	1.10	0.46	12.00	0.80	0.33	5.00
Mar 2024	1.60	0.05	9.00	3.10	0.04	11.00	1.20	0.12	18.00	1.90	0.46	19.00	1.10	0.03	10.00
Apr 2024	1.76	0.10	5.00	3.41	BDL [#]	5.00	1.32	0.10	12.00	2.09	0.50	14.00	1.21	BDL [#]	4.00
May 2024	0.88	BDL [#]	5.00	1.69	BDL [#]	6.00	0.67	0.10	10.00	1.05	0.30	10.00	0.61	BDL [#]	3.00
Aug 2024	1.90	0.03	6.00	2.71	0.04	7.00	1.68	0.80	11.00	2.06	0.09	11.00	1.63	BDL [#]	7.00
Sep 2024	17.60	0.80	32.00	18.40	0.80	31.00	10.60	1.20	25.00	21.90	2.10	40.00	14.60	0.75	29.00
Oct 2024	9.60	0.90	31.00	10.10	0.75	31.00	9.40	1.00	24.00	16.50	2.10	41.00	4.60	0.50	24.00
Nov 2024	9.60	0.80	25.00	9.20	0.75	25.00	8.20	0.60	21.00	15.50	1.60	38.00	4.50	0.40	16.00
Dec 2024	9.00	0.75	24.00	8.20	0.70	24.00	7.00	0.40	19.00	14.00	1.60	31.00	4.60	0.30	12.00
Jan 2025	8.30	0.73	20.00	8.30	0.68	18.00	3.00	0.20	15.00	14.20	1.45	15.00	4.60	0.20	12.00
Feb 2025	4.80	0.62	16.00	5.50	0.53	18.00	2.50	0.18	15.00	9.80	1.00	15.00	4.60	0.20	12.00
Mar 2025	8.2	0.68	14.00	8.8	0.68	14.00	4	0.2	15.00	7.3	0.79	15.00	8	0.4	12.00

[#] Values reported as BDL indicate concentrations below the analytical detection limit and do not represent true zeros.

Nitrate, phosphate and sulfate concentrations significantly increased post-storm for most of the sites (Figure 3). Nitrate concentrations exhibited a marked and statistically consistent elevation in the post-hurricane period across all sampling sites, underscoring the vulnerability of the watershed's nitrogen pools to hydrological disturbance. At Firefly Trail (FT), nitrate rose from a pre-storm mean of 1.67 ± 0.45 mg/L to 9.59 ± 3.61 mg/L post-storm, with the maximum value increasing from 2.40 to 17.60 mg/L. River Mill (RM) showed a similar pattern, with mean nitrate concentrations increased from 2.56 ± 0.66 mg/L in pre-storm events to 9.79 ± 3.75 mg/L in post-storm events, and a maximum rise from 3.41 to 18.40 mg/L. Sandy Creek (SC), though a lentic system, also reflected this surge, increasing from 1.10 ± 0.43 mg/L in pre-storm events to 6.39 ± 2.99 mg/L in post-storm events, with a maximum rise from 1.68 to 10.60 mg/L. At the Water Treatment Plant (WTP), nitrate rose from 1.16 ± 0.37 mg/L in pre-storm events to 6.50 ± 3.51 mg/L in post-storm events, with a maximum rise from 1.63 to 14.60 mg/L. While the Oconee River (OR) experienced the most pronounced increase in pre-storm events from 1.70 ± 0.44 mg/L to 14.17 ± 4.36 mg/L in post-storm events, with a maximum rise from 2.09 to 21.90 mg/L (Table 3). These data reflect a consistent post-disturbance increase in mean and variability, suggesting the influence of storm-enhanced connectivity, runoff, and possible legacy nitrogen mobilization. Although concentrations have declined gradually in the weeks following the Hurricane, nitrate levels remain significantly above pre-storm baselines, indicating a slow system recovery.

Phosphate concentrations responded with equally substantial spatial heterogeneity and sharp post-storm increases, particularly in areas with high sediment mobility and anthropogenic inputs. FT saw phosphate increase from a pre-storm mean of 0.11 ± 0.09 mg/L to post-storm 0.75 ± 0.08 mg/L, with the maximum rising from 0.28 to 0.90 mg/L. RM followed closely, increasing from 0.06 ± 0.08 mg/L in pre-storm events to 0.70 ± 0.07 mg/L in post-storm events, with a maximum rising from 0.24 to 0.80 mg/L. SC, while already elevated pre-storm (mean: 0.29 ± 0.26 mg/L), rose further to 0.54 ± 0.38 mg/L in post-storm events, likely due to localized urban and parkland runoff, with a maximum rising from 0.80 to 1.20 mg/L. WTP showed an increase from 0.11 ± 0.13 mg/L to 0.39 ± 0.17 mg/L. The most substantial change occurred at OR, where phosphate rose from 0.32 ± 0.16 mg/L in pre-storm events to 1.52 ± 0.46 mg/L in post-storm events, with a maximum rising from 0.50 to 2.10 mg/L (Table 3). These post-storm surges in phosphorus are likely to reflect remobilization of sediment-bound phosphorus and increased urban stormwater discharge. Unlike nitrates, phosphate appears to attenuate more rapidly over time, potentially due to re-sedimentation, sorption, and biological uptake.

Sulfate concentrations across the watershed also increased substantially after the Hurricane, with high values recorded in urban, agricultural, and forest areas. At FT, sulfate increased from 7.00 ± 1.73 mg/L in pre-storm events to 23.14 ± 6.42 mg/L in post-storm events, with a maximum rising from 9 to 32 mg/L. In comparison, RM rose from 7.20 ± 2.03 mg/L in pre-storm events to 23 ± 6.14 mg/L in post-storm events, with a maximum increase from 11 to 31 mg/L. SC, which showed relatively high pre-storm levels (13.67 ± 2.86 mg/L), rose to 19.14 ± 4.01 mg/L, with a maximum rising from 18 to 25 mg/L. WTP showed an increase from 7.50 ± 4.42 mg/L in pre-storm events to 16.71 ± 6.47 mg/L in post-storm events, with a maximum rising from 16 to 29 mg/L. OR previously showed 14.00 ± 3.41 mg/L during pre-storm events, increasing to 27.86 ± 11.51 mg/L in post-storm events, with a maximum rising from 19 to 41 mg/L (Table 3, Figure 3). These patterns suggest widespread mobilization of sulfur compounds, potentially from the decomposition of organic matter, fertilizer residues, and infrastructure infiltration. The elevated standard deviations across all sites post-storm also point to increased spatial-temporal variability and episodic sulfate release.

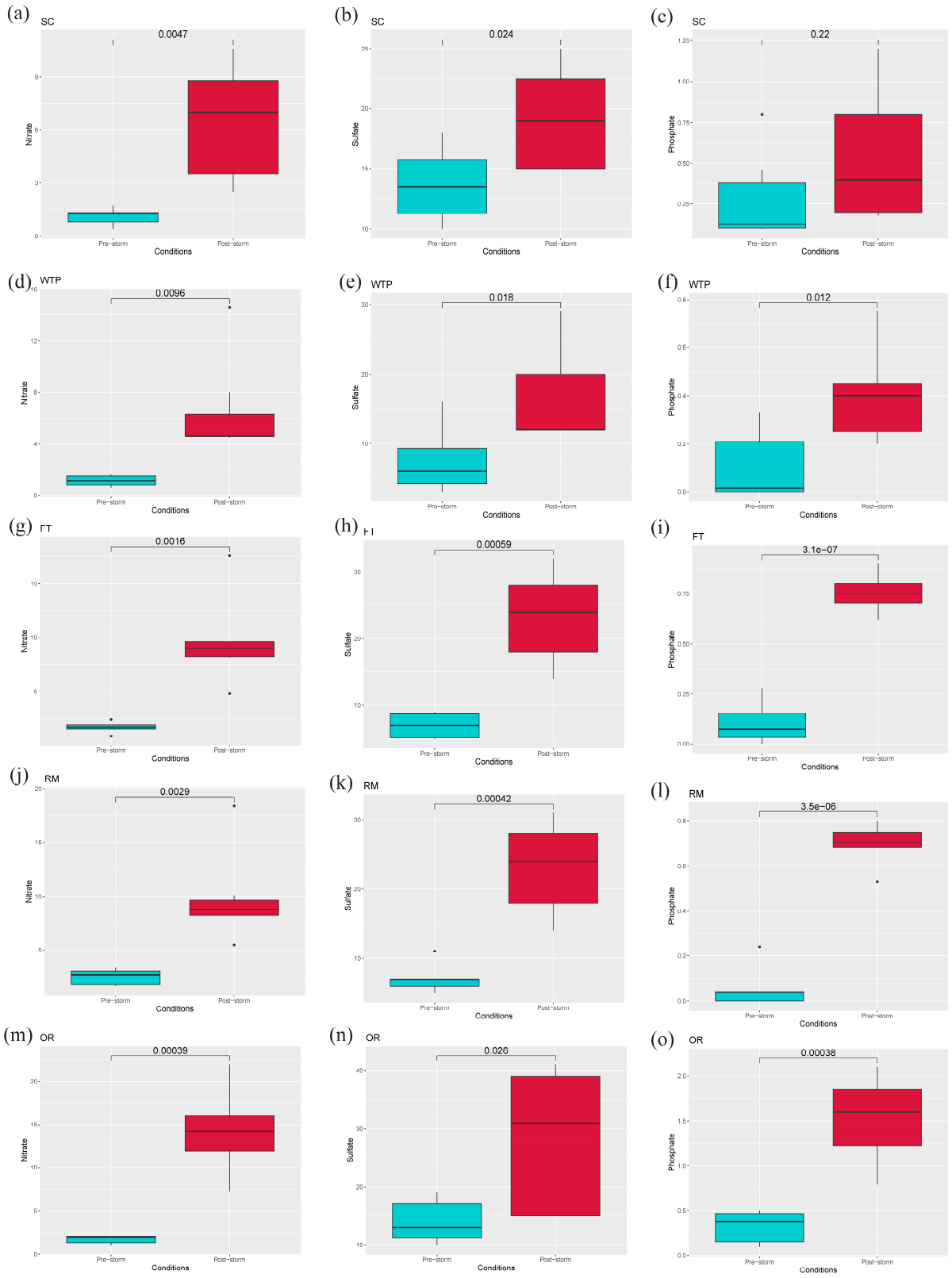


Figure 3. Boxplot illustrating the shifts in nitrate, phosphate and sulfate concentrations between pre-storm and post-storm events. A pairwise comparison for significance was conducted using *t*-test. The boxplot sampling locations within the Oconee River watershed. Panels (**a**–**c**) represent Sandy Creek (SC), a lentic recreational system; (**d**–**f**) Water Treatment Plant in-take (WTP) on the North Oconee River; (**g**–**i**) Firefly Trail (FT), an urbanized river reach; (**j**–**l**) River Mill (RM), a down-stream urban reach; and (**m**–**o**) the Oconee River mainstem (OR).

3.2. Correlation Structure and Nutrient–Hydrology Coupling

During pre-storm events, nitrate exhibited a very weak correlation with discharge across sites, indicating minimal hydrologic control under baseflow conditions. Phosphate showed a broader but still inconsistent range of correlations, reflecting site-specific interplay between particulate inputs, groundwater dilution, and sediment exchange. Sulfate, by contrast, showed consistently strong positive pre-storm correlations with discharge, indicating stable hydrologic sourcing from groundwater, existing surface runoff, and possible mineral weathering. After the storm event, nitrate–discharge correlations increased across all sites, indicating a transition to rapid, event-driven nitrate flushing primarily from surface runoff. Phosphate–discharge correlations also shifted upward, becoming uniformly positive, indicating enhanced hydrologic mobilization of dissolved and particulate phosphorus. Sulfate–discharge correlations weakened but remained positive, suggesting that while hydrologic transport remained important, a possible storm-induced redox shift increasingly influenced sulfate concentration (Figure 4, Supplementary Information-S2). To facilitate interpretation at both watershed and site scales, Figure 4 presents aggregated correlation patterns across all monitoring locations, while site-specific correlation matrices are provided in Supplementary Information-S2.

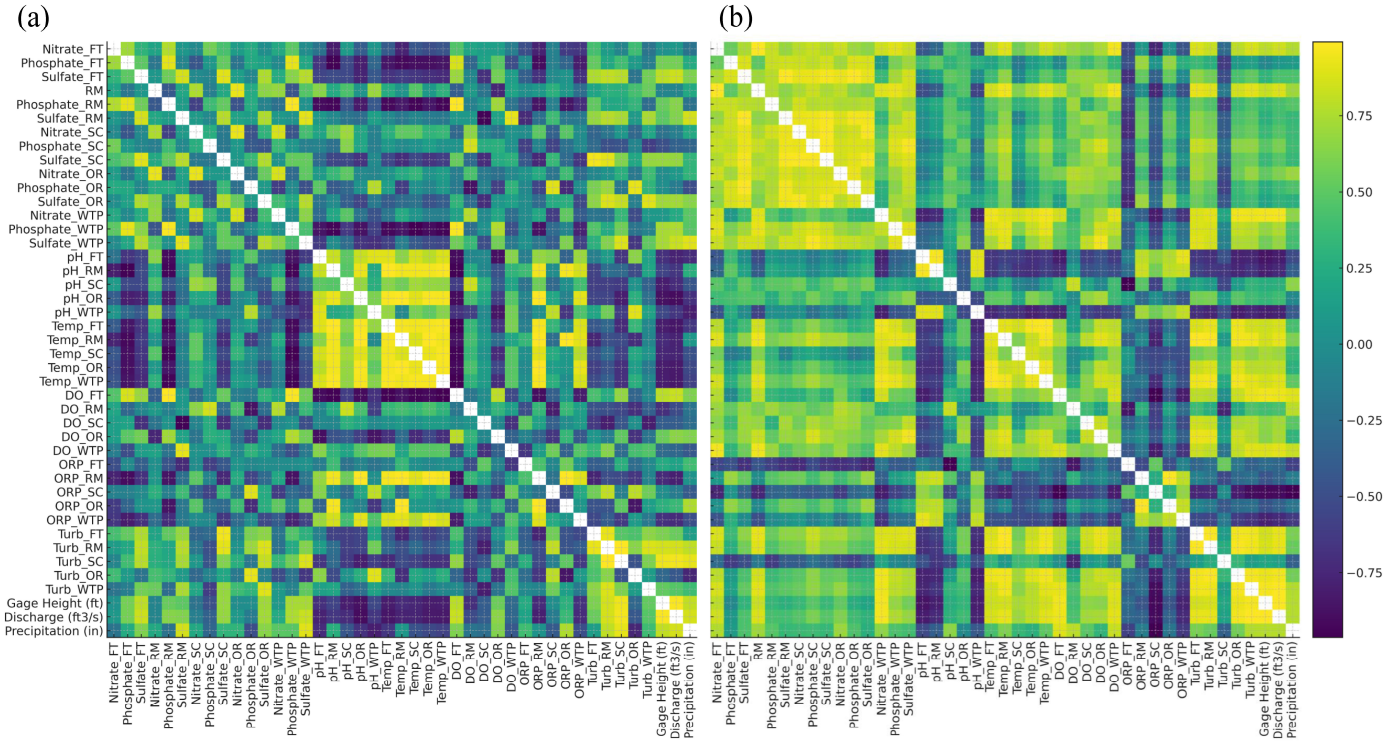


Figure 4. Heatmaps of Pearson correlation coefficients illustrating pairwise relationships among nutrients (nitrate, phosphate, sulfate), physicochemical parameters (pH, temperature [Temp], DO, ORP, turbidity [Turb]), and hydrologic drivers (gage height, discharge, precipitation) across monitoring stations before and after the storm event. Panel (**a**) shows pre-storm correlations and panel (**b**) shows post-storm correlations.

Before the storm, nitrate showed weak, inconsistent correlations with turbidity, consistent with its dominant dissolved form and limited affinity for particulate transport. Phosphate, however, displayed a much wider pre-storm range, with several sites showing strong positive relationships indicative of phosphorus' known association with sediment-bound phases. Sulfate exhibited moderately positive but variable pre-storm turbidity correlations, reflecting contributions from both dissolved and particle-associated pools.

After the storm, nitrate–turbidity correlations strengthened positively at most sites, suggesting that stormflow mobilized nitrate stored near the surface and transported it along with suspended sediments. Phosphate–turbidity correlations also became uniformly positive in the post-storm period, reflecting sediment resuspension during high flows and the possible subsequent desorption of phosphorus from sediment particles. Sulfate–turbidity correlations became more heterogeneous, indicating that stormflows promoted dissolved sulfate sources at some sites while amplifying particulate associations at others (Figure 4, Supplementary Information-S2). Across all correlation coefficients, the lentic system (SC) showed a distinctly different pre- and post-storm response compared with the lotic systems (WTP, FT, RM, OR).

Based on the observed changes in nutrient–pH and nutrient–ORP relationships, several potential explanations emerge for how stormflow altered the geochemical controls on nutrient mobility. Under pre-storm conditions, relatively stable pH and redox environments likely governed nutrient behavior, with nitrate responding inconsistently across sites, phosphate showing strong sensitivity to acidic conditions, and sulfate reflecting acid–base influences on dissolution. After the storm, these relationships shifted noticeably. One possible reason for the stronger negative correlation between nitrate and pH at several sites is the influx of acidic runoff, which may have mobilized surface-derived nitrate. The reduced or reversed pH dependence of phosphate following the storm may indicate that high-flow conditions weakened normal sorption constraints by disturbing sediments and altering equilibrium chemistry. The more variable sulfate–pH patterns observed post-storm could result from site-specific changes in acidity and enhanced oxidation. Nutrient–ORP relationships also reorganized, whereas phosphate and sulfate were more closely correlated with reducing conditions before the storm, several sites showed stronger positive associations with ORP afterward. This may reflect the influence of more oxidizing stormwaters, which can promote nitrate transport, enhance the oxidation of reduced sulfur pools, and modify phosphorus release mechanisms. The results suggest that stormflow shifted nutrient regulation away from stable, baseflow geochemical controls toward more dynamic pathways shaped by storm-driven changes in acidity and redox state.

3.3. Early Recovery and Solute-Specific Attenuation

Declines in nutrient concentrations were observed within 8–16 weeks post-storm, but recovery trajectories differed among ions and across sites. Phosphate exhibited the fastest attenuation, returning to near pre-disturbance means at FT and WTP by ~60–75 days post-Helene. This rapid decline is consistent with post-event deposition of fine sediments, particle settling in lower velocity reaches (SC), and biological uptake. In contrast, nitrate reductions were slower and more variable. OR and RM displayed continued episodic peaks after baseflow resumed, potentially indicating delayed delivery from riparian soil and disturbed near-stream aquifers. Sulfate exhibited the most prolonged post-storm response among the three solutes. Concentrations increased sharply at all sites immediately following the storm, but unlike nitrate and phosphate, sulfate did not return to pre-storm conditions during the hydrologic recession. At OR and FT, sulfate remained elevated from October 2024 through March 2025 in most of the sites, despite discharge returning to baseline shortly after the storm peak. This pattern indicates that possible hydrologic normalization did not coincide with chemical stabilization, and that sulfate export continued under baseflow conditions throughout the winter sampling period. In contrast, SC, RM, and WTP displayed attenuation toward pre-storm levels but still maintained higher variability than observed before the Hurricane.

4. Discussion

The results demonstrate that Hurricane Helene induced a watershed-scale shift in nutrient transport and biogeochemical function despite the absence of visible geomorphic alteration. Precipitation associated with the storm produced a rapid rise in discharge and gage height at the North Oconee River USGS station, indicating sharp increases in hydrologic connectivity, defined here as the storm-driven activation of surface runoff and shallow subsurface flow pathways that link upland, riparian, and urban source areas to the stream network across the watershed. This hydrologic response was followed by a pronounced increase in dissolved and particle-bound solutes at all sites. The magnitude of these changes is comparable to nutrient pulses documented in southeastern and Mid-Atlantic River systems following short-duration, high-intensity precipitation [40]. Most previous reports focus on overbank flooding or channel erosion; in contrast, the Oconee watershed experienced elevated discharge without significant flooding, showing that hydrologic disturbance alone can reorganize solute transport pathways.

4.1. Divergent Source Pools and Transport Mechanisms Regulating Post-Hurricane Nutrient Export

The ions investigated in this study respond to storm forcing through distinct physicochemical pathways. Nitrate exhibited strong positive correlations with discharge following the precipitation pulse associated with Hurricane Helene, indicating that transport was dominated by rapid surface-flushing rather than by groundwater contribution. The highest nitrate concentrations occurred on 30 September 2024, coincident with peak discharge and maximum gage height, and elevated variance persisted during the early recession period. This pattern is consistent with the mobilization of legacy nitrogen from riparian soils and near-stream subsurface horizons when hydraulic gradients increase during storm infiltration. The subsequent gradual decline in nitrate concentrations is possibly due to delayed leaching and continued shallow subsurface transport, a behavior commonly observed in mixed land-use basins following high-intensity rainfall [41]. Phosphate exhibited a different response pattern. Peak concentrations aligned with increased discharge and elevated turbidity immediately after the storm, indicating that phosphorus mobilization was driven by particulate and sediment-associated pathways. The strong phosphate–turbidity relationship during the post-storm period is consistent with resuspension of phosphorus-bearing sediments and desorption under transient redox or pH fluctuations [42]. As discharge and gage height declined in subsequent sampling cycles, phosphate concentrations decreased rapidly, suggesting attenuation through sediment settling, mineral sorption, and biological uptake [43].

Sulfate diverged from both nitrate and phosphate. Although sulfate increased sharply at the storm peak, concentrations did not decline following hydrologic recession. At the Oconee River and Firefly Trail sites, sulfate remained elevated from October 2024 through March 2025, even after discharge and gage height returned to baseline. As streamflow returned to normal while sulfate did not, it suggests the sulfate was coming from dissolved sulfur sources rather than from particles being washed in. The weak correlation with turbidity supports a dissolved-phase mechanism involving soil-water flushing and redox-mediated mobilization [44]. Urban and agricultural inputs may also contribute to this prolonged signal. The persistence of sulfate under baseflow conditions shows that a uniform decline cannot represent nutrient recovery, and that storm impacts extend into the post-event period [45].

4.2. Hydrologic Homogenization Across Land-Use Gradients

Under baseflow conditions, nutrient concentrations reflect established land-use patterns, with urban reaches exhibiting consistently higher nitrate and phosphate concentra-

tions than in forest areas or lentic sites [45]. The precipitation–discharge event associated with Helene temporarily reduced these spatial gradients. All sites showed simultaneous increases in nitrate, phosphate, and sulfate during peak discharge, indicating hydrologic homogenization. This behavior reflects a shift from localized source control to watershed-scale flushing, in which elevated hydraulic gradients mobilize solutes from multiple source pools. Similar homogenization has been reported for dissolved organic carbon and inorganic nitrogen during extreme rainfall events, where cross-catchment hydrologic connectivity causes rapid redistribution of solutes [46]. Results from the Oconee watershed indicate that homogenization occurs in the absence of channel flooding, showing that nutrient exports can be reorganized solely by short-duration, high-intensity rainfall.

4.3. Persistence of Disturbance Effects During Hydrologic Recession

Although discharge and gage height returned to baseline within weeks of the storm, solute recovery lagged behind hydrologic stabilization. Nitrate and sulfate maintained elevated concentrations across multiple sampling events during low-flow conditions, demonstrating that chemical responses extended well beyond the physical forcing period. This temporal change suggests continued subsurface release and biogeochemical processing initiated during storm infiltration [6]. Transient post-storm increases in nitrate and sulfate occurred during periods without visible disturbance, making them unlikely to be detected by infrequent monitoring or discharge-only assessments. The results from this watershed show that event-responsive sampling is required to characterize post-storm solute export. These results have direct implications for environmental monitoring design. The persistence of elevated nutrient concentrations under post-storm low-flow conditions indicates that water-quality responses may extend beyond peak discharge, such that routine low-frequency or discharge-triggered monitoring is likely to underestimate storm-driven nutrient exports. As extreme precipitation events intensify, targeted sampling during storm and recovery periods will be increasingly important for resolving nutrient transport pathways and informing adaptive watershed management. Low-frequency sampling intervals would not have captured the magnitude or duration of the nutrient perturbations observed here and may not fully represent biogeochemical responses to short-lived hydrologic disturbances. Although storm-induced increases in nutrient concentrations clearly indicate enhanced watershed exports following Hurricane Helene 2024, quantitative estimation of total nutrient fluxes was not feasible due to the absence of site-specific continuous discharge data. Future studies integrating high-frequency nutrient sampling with co-located discharge measurements would allow direct calculation of storm-driven nutrient loads and facilitate comparison across watersheds and storm events. This study is best interpreted as a process-focused case study, providing mechanistic insight into storm-driven nutrient dynamics rather than predictive generalization across all storm types or watershed settings.

5. Conclusions

Hurricane Helene generated pronounced shifts in nutrient dynamics within the Oconee River watershed despite minimal visible geomorphic alteration. Increases in discharge initiated rapid mobilization of nitrate, phosphate, and sulfate from distinct source pools, resulting in solute behavior that departed markedly from pre-storm patterns [47]. Based on the results, nitrate was transported primarily through shallow subsurface flushing and delayed release from riparian soils; phosphate was mobilized through particulate resuspension and mineral desorption; and sulfate exhibited a sustained elevation associated with dissolved-phase pathways and redox-mediated mobilization. These differentiated trajectories make clear that watershed biogeochemistry is inherently storm-responsive and will undergo measurable, often substantial, alteration following high-intensity precipitation

events, even when physical disturbance appears limited [48]. Similar to recent findings that external stressors can restructure aquatic biogeochemical processes by altering microbial community function, the results from the present study highlight that disturbances, whether storm-driven or contaminant-driven, can trigger rapid shifts in nutrient cycling pathways [49]. Event-driven hydrologic connectivity temporarily homogenized spatial nutrient patterns across heterogeneous land-use settings, indicating that short-duration, high-intensity rainfall can reorganize export pathways even in catchments that exhibit no overt flood damage. The persistence of elevated solute concentrations well beyond the hydrologic recession further indicates that chemical responses extend over longer timescales than the physical forcing event that initiates them. These findings emphasize the need for high-frequency sampling strategies capable of resolving short-term hydrologic and biogeochemical perturbations. Reliance on low-resolution monitoring would capture only a partial representation of the magnitude, duration, and solute-specific nature of post-storm responses. For regions where legacy nutrient stores, heterogeneous land use, and engineered drainage infrastructure intersect, such event-scale approaches are essential for accurately characterizing watershed resilience, nutrient export trajectories, and surface-water quality [50]. The results demonstrate that even short-lived hydrologic disturbances can exert disproportionate influence on nutrient fluxes, underscoring the need to integrate event-responsive monitoring into long-term watershed assessment frameworks.

Supplementary Materials: The following supporting information can be downloaded at: https://www.mdpi.com/article/10.3390/environments13020076/s1, Supplementary Information-S1 Table S1: Descriptive statistics of nitrate, phosphate, and sulfate concentrations across all locations from January 2024–March 2025, Supplementary Information-S2, Excel spreadsheet of correlation matrix, correlation matrix prestorm, correlation matrix post storm.

Author Contributions: A.B. and G.S. are co-first authors and contributed equally to this work. They jointly conducted the laboratory analyses, with G.S. leading the pre-storm data analyses and A.B. leading the post-storm data analyses. Both authors contributed to statistical analyses and wrote the initial draft of the manuscript. In future citations or CV listings, either A.B. or G.S. may appear as first author. B.M. and G.B. assisted with sample collection and supported laboratory analyses and provided a review of the manuscript. A.D. and S.D. conceived the idea, supervised the study, provided resources, and contributed to writing and revising the manuscript. All authors have read and agreed to the published version of the manuscript.

Funding: This research was funded by the National Science Foundation under Award No. EAR-2502654. This research was partially supported by the U.S. Department of Energy, Office of Environmental Management, under Award No. DE-EM0005228 to the University of Georgia Research Foundation.

Data Availability Statement: The original contributions presented in this study are included in the article/Supplementary Materials. Further inquiries can be directed to the corresponding author.

Acknowledgments: The authors wish to express their gratitude to William Cottrell and Tiger Brook from J.G. Beacham Water Treatment Plant in Athens, Clarke County, for their continuous assistance and support in obtaining water samples from the North Oconee River near the Water Treatment Plant. The authors would also like to extend their sincere thanks to Rose West, from Nature Division, at the Athens-Clarke County Leisure Services Department, for granting permission to collect samples from the North Oconee River at the Greenway near the Firefly Trail in Athens, as well as at Sandy Creek Beach Park near Lake Chapman.

Conflicts of Interest: The authors declare no conflict of interest.

References

1. Vidon, P.; Karwan, D.L.; Andres, A.S.; Inamdar, S.; Kaushal, S.; Morrison, J.; Mullaney, J.; Ross, D.S.; Schroth, A.W.; Shanley, J.B.; et al. In the path of the Hurricane: Impact of Hurricane Irene and Tropical Storm Lee on watershed hydrology and biogeochemistry from North Carolina to Maine, USA. *Biogeochemistry* **2018**, *141*, 351–364. [CrossRef]
2. Juan-Diego, E.; Mendoza, A.; Arganis-Juárez, M.L.; Berezowsky-Verduzco, M. Alteration of Catchments and Rivers, and the Effect on Floods: An Overview of Processes and Restoration Actions. *Water* **2025**, *17*, 1177. [CrossRef]
3. Meixner, T.; Huth, A.K.; Brooks, P.D.; Conklin, M.H.; Grimm, N.B.; Bales, R.C.; Haas, P.A.; Petti, J.R. Influence of shifting flow paths on nitrogen concentrations during monsoon floods, San Pedro River, Arizona. *J. Geophys. Res. Biogeosci.* **2007**, *112*, G03S03.
4. Stamm, G.; Bhattacharjee, A.; Basapuram, G.; Dutta, A.; Duttagupta, S. Molecular and Ionic Signatures in Rainwater: Unveiling Sources of Atmospheric Pollution. *Environments* **2025**, *12*, 351. [CrossRef]
5. Heiler, G.; Hein, T.; Schiemer, F.; Bornette, G. Hydrological connectivity and flood pulses as the central aspects for the integrity of a river-floodplain system. *Regul. Rivers Res. Manag.* **1995**, *11*, 351–361. [CrossRef]
6. McMillan, S.K.; Wilson, H.F.; Tague, C.L.; Hanes, D.M.; Inamdar, S.; Karwan, D.L.; Loecke, T.; Morrison, J.; Murphy, S.F.; Vidon, P. Before the storm: Antecedent conditions as regulators of hydrologic and biogeochemical response to extreme climate events. *Biogeochemistry* **2018**, *141*, 487–501. [CrossRef]
7. Lu, A. Stress and physical health deterioration in the aftermath of Hurricanes Katrina and Rita. *Sociol. Perspect.* **2011**, *54*, 229–250. [CrossRef]
8. Lugo, A.E. Visible and invisible effects of hurricanes on forest ecosystems: An international review. *Austral Ecol.* **2008**, *33*, 368–398. [CrossRef]
9. Paerl, H.W.; Crosswell, J.R.; Van Dam, B.; Hall, N.S.; Rossignol, K.L.; Osburn, C.L.; Hounshell, A.G.; Sloup, R.S.; Harding, L.W., Jr. Two decades of tropical cyclone impacts on North Carolina's estuarine carbon, nutrient and phytoplankton dynamics: Implications for biogeochemical cycling and water quality in a stormier world. *Biogeochemistry* **2018**, *141*, 307–332. [CrossRef]
10. Cai, Y.; Guo, L.; Wang, X.; Lohrenz, S.E.; Mojzis, A.K. Effects of tropical cyclones on river chemistry: A case study of the lower Pearl River during Hurricanes Gustav and Ike. *Estuar. Coast. Shelf Sci.* **2013**, *129*, 180–188. [CrossRef]
11. Plomaritis, T.A.; Ferreira, Ó.; Costas, S. Regional assessment of storm related overwash and breaching hazards on coastal barriers. *Coast. Eng.* **2018**, *134*, 124–133. [CrossRef]
12. Ma, H.; Xu, L.; Okon, S.U.; Hu, P.; Li, W.; Shi, H.; He, Z. Sediment transport and bed erosion during storm surge using a coupled hydrodynamic and morphodynamic model considering wave and current interaction. *Coast. Eng.* **2024**, *187*, 104409. [CrossRef]
13. Nienhuis, J.H.; Heijkers, L.G.; Ruessink, G. Barrier breaching versus overwash deposition: Predicting the morphologic impact of storms on coastal barriers. *J. Geophys. Res. Earth Surf.* **2021**, *126*, e2021JF006066. [CrossRef]
14. Gori, A.; Lin, N.; Xi, D. Tropical cyclone compound flood hazard assessment: From investigating drivers to quantifying extreme water levels. *Earth's Future* **2020**, *8*, e2020EF001660. [CrossRef]
15. Ma, M. Numerical Modeling of Hurricane Wave and Storm Surge Overtopping Sand Dunes and Barrier Island. 2024. Available online: https://repository.lib.fsu.edu/islandora/object/fsu:932610/datastream/PDF/view (accessed on 26 January 2026).
16. Hagen, A.B. The 2024 Atlantic Hurricane Season: Helene and Milton Highlight Five US Hurricane Landfalls. *Weatherwise* **2025**, *78*, 19–28. [CrossRef]
17. Watson, P.J. Influence of Major Hurricanes "Helene" and "Milton" in 2024 on EVA of the Long Ocean Water Level Record at Key West, USA. *Coasts* **2025**, *5*, 41. [CrossRef]
18. Price, A.P. *The Effect of Climate and Land Use on the Hydrology of the Upper Oconee River Basin, Georgia*; University of California: Los Angeles, LA, USA, 1998.
19. Speir, S.L.; Tank, J.L.; Bieroza, M.; Mahl, U.H.; Royer, T.V. Storm size and hydrologic modification influence nitrate mobilization and transport in agricultural watersheds. *Biogeochemistry* **2021**, *156*, 319–334. [CrossRef]
20. Wohl, E. An integrative conceptualization of floodplain storage. *Rev. Geophys.* **2021**, *59*, e2020RG000724. [CrossRef]
21. Sánchez-Arcilla, A.; Garrote, L.; Gracia, V.; Cáceres, I.; Sánchez-Artús, X.; Caiola, N.; Espanya, A.; Espino, M.; García, M.Á.; Grassa, J.M.; et al. Trade-offs and synergies in river-coastal restoration for the Ebro case (Spanish Mediterranean). *Nat. Conserv.* **2025**, *59*, 101–137. [CrossRef]
22. Moravcová, J.; Pavlíček, T.; Ondr, P.; Koupilová, M.; Kvítek, T. Comparison of parameters influencing the behavior of concentration of nitrates and phosphates during different extreme rainfall-runoff events in small watersheds. *Hydrol. Earth Syst. Sci. Discuss.* **2013**, *10*, 12105–12151.
23. Newcomer Johnson, T.A.; Kaushal, S.S.; Mayer, P.M.; Grese, M.M. Effects of stormwater management and stream restoration on watershed nitrogen retention. *Biogeochemistry* **2014**, *121*, 81–106. [CrossRef]
24. Goldberg, S.; Sposito, G. On the mechanism of specific phosphate adsorption by hydroxylated mineral surfaces: A review. *Commun. Soil Sci. Plant Anal.* **1985**, *16*, 801–821. [CrossRef]
25. Li, X.; Gan, Y.; Zhou, A.; Liu, Y. Relationship between water discharge and sulfate sources of the Yangtze River inferred from seasonal variations of sulfur and oxygen isotopic compositions. *J. Geochem. Explor.* **2015**, *153*, 30–39. [CrossRef]

26. Pastuszak, M.; Witek, Z.; Nagel, K.; Wielgat, M.; Grelowski, A. Role of the Oder estuary (southern Baltic) in transformation of the riverine nutrient loads. *J. Mar. Syst.* **2005**, *57*, 30–54. [CrossRef]
27. Burns, D.A.; Pellerin, B.A.; Miller, M.P.; Capel, P.D.; Tesoriero, A.J.; Duncan, J.M. Monitoring the riverine pulse: Applying high-frequency nitrate data to advance integrative understanding of biogeochemical and hydrological processes. *Wiley Interdiscip. Rev. Water* **2019**, *6*, e1348. [CrossRef]
28. Chen, S.; Lu, Y.; Dash, P.; Das, P.; Li, J.; Capps, K.; Majidzadeh, H.; Elliott, M. Hurricane pulses: Small watershed exports of dissolved nutrients and organic matter during large storms in the Southeastern USA. *Sci. Total Environ.* **2019**, *689*, 232–244. [CrossRef]
29. Duttagupta, S.; Basapuram, G.; Cottrell, W.; Dutta, A. Landuse and land cover shape organic contaminants distribution in the Oconee River watershed in Georgia. *npj Emerg. Contam.* **2025**, *1*, 3. [CrossRef]
30. Stamm, G.; Basapuram, G.; Duttagupta, S.; Dutta, A. Anion-mediated pathways in organophosphate degradation in the Oconee River watershed in Georgia. *Emerg. Contam.* **2025**, *11*, 100542. [CrossRef]
31. Amorim, R.; Villarini, G.; Czajkowski, J.; Smith, J. Flooding from Hurricane Helene and associated impacts: A historical perspective. *J. Hydrol. X* **2025**, *27*, 100204. [CrossRef]
32. Anarde, K.A.; Kameshwar, S.; Irza, J.N.; Nittrouer, J.A.; Lorenzo-Trueba, J.; Padgett, J.E.; Sebastian, A.; Bedient, P.B. Impacts of hurricane storm surge on infrastructure vulnerability for an evolving coastal landscape. *Nat. Hazards Rev.* **2018**, *19*, 04017020. [CrossRef]
33. Callaghan, J. Disastrous Effects of Hurricane Helene in the Southern Appalachian Mountains Including a Review of Mechanisms Producing Extreme Rainfall. *Hydrology* **2025**, *12*, 201. [CrossRef]
34. Basapuram, G.; Duttagupta, S.; Dutta, A. Detection and screening of organic contaminants in A riverine system of Georgia using non-targeted analysis. *Environments* **2024**, *11*, 89. [CrossRef]
35. US Geological Survey (USGS). USGS Monitoring Location 02217500, Middle Oconee River near Athens, Georgia: Continuous Stream-Gage Data (Parameter 00065). 2025. Available online: https://waterdata.usgs.gov/monitoring-location/USGS-02217500/#dataTypeId=continuous-00065-0&period=P7D&showFieldMeasurements=true (accessed on 13 November 2025).
36. NOAA. OCNG1—Oconee River near Davisboro, Georgia: Real-Time Water-Level/Gauge Data. 2025. Available online: https://water.noaa.gov/gauges/ocng1 (accessed on 13 November 2025).
37. US Geological Survey. Annual NLCD (National Land Cover Database)—The Next Generation of Land Cover Mapping (Fact Sheet 2025-3001). 2025. Available online: https://www.usgs.gov/centers/eros/science/national-land-cover-database#data (accessed on 13 November 2025).
38. Bonnell, J.; Ogihara, M. *Exploring Data Science with R and the Tidyverse: A Concise Introduction*; Chapman and Hall/CRC: New York, NY, USA, 2023.
39. Harrell, F.E., Jr.; Harrell, M.F., Jr. Package 'hmisc'. *CRAN2018* **2019**, *2019*, 235–236.
40. Kemper, J.T.; Miller, A.J.; Welty, C. Spatial and temporal patterns of suspended sediment transport in nested urban watersheds. *Geomorphology* **2019**, *336*, 95–106. [CrossRef]
41. McAleer, E.; Coxon, C.; Mellander, P.E.; Grant, J.; Richards, K. Patterns and drivers of groundwater and stream nitrate concentrations in intensively managed agricultural catchments. *Water* **2022**, *14*, 1388. [CrossRef]
42. Blanco, A.C.; Nadaoka, K.; Yamamoto, T.; Kinjo, K. Dynamic evolution of nutrient discharge under stormflow and baseflow conditions in a coastal agricultural watershed in Ishigaki Island, Okinawa, Japan. *Hydrol. Process.* **2010**, *24*, 2601–2616. [CrossRef]
43. Bowes, M.J.; House, W.A.; Hodgkinson, R.A.; Leach, D.V. Phosphorus–discharge hysteresis during storm events along a river catchment: The River Swale, UK. *Water Res.* **2005**, *39*, 751–762. [CrossRef]
44. Kivi, S.T.; Bailey, R.T. Modeling sulfur cycling and sulfate reactive transport in an agricultural groundwater system. *Agric. Water Manag.* **2017**, *185*, 78–92. [CrossRef]
45. Tromboni, F.; Dodds, W.K. Relationships between land use and stream nutrient concentrations in a highly urbanized tropical region of Brazil: Thresholds and riparian zones. *Environ. Manag.* **2017**, *60*, 30–40. [CrossRef]
46. Basu, N.B.; Thompson, S.E.; Rao, P.S. Hydrologic and biogeochemical functioning of intensively managed catchments: A synthesis of top-down analyses. *Water Resour. Res.* **2011**, *47*, ARTN-W00J15. [CrossRef]
47. Huang, S.; Sherman, A.; Chen, C.; Jaffé, P.R. Tropical cyclone effects on water and sediment chemistry and the microbial community in estuarine ecosystems. *Environ. Pollut.* **2021**, *286*, 117228. [CrossRef] [PubMed]
48. Geyer, N.; Huettel, M.; Wetz, M. Biogeochemistry of a river-dominated estuary influenced by drought and storms. *Estuaries Coasts* **2018**, *41*, 2009–2023. [CrossRef]

49. Basapuram, G.; Duttagupta, S.; Dutta, A. Pesticides impact microbial communities in the freshwater ecosystem: Implications on biogeochemical cycles. *J. Hazard. Mater.* **2025**, *500*, 140403. [CrossRef] [PubMed]
50. Windham-Myers, L.; Root, T.L.; Petkewich, M.D.; Musgrove, M.; Gill, A.C.; Weaver, J.C.; Conaway, C.H.; Lindsey, B.D.; Parchaso, F.; Knowles, N.; et al. *State of Science, Gap Analysis, and Prioritization for Southeastern United States Water-Quality Impacts from Coastal Storms—Fiscal Year 2023 Program Report to the Water Resources Mission Area from the Water Availability Impacts of Extreme Events Program—Hurricanes*; US Geological Survey: Reston, VA, USA, 2024.

Disclaimer/Publisher's Note: The statements, opinions and data contained in all publications are solely those of the individual author(s) and contributor(s) and not of MDPI and/or the editor(s). MDPI and/or the editor(s) disclaim responsibility for any injury to people or property resulting from any ideas, methods, instructions or products referred to in the content.